08

Microwave magnetoresistance effect in a (CoFe/Cu) superlattice with micron-sized holes

© *A.B. Rinkevich,*[1] *M.A. Milyaev,*[1] *E.A. Kuznetsov,*[1,2] *D.V. Perov,*[1] *A.Yu. Pavlova*[1]

[1] M.N. Mikheev Institute of Metal Physics, Ural Branch, Russian Academy of Sciences,
Yekaterinburg, Russia
[2] Russian State Vocational Pedagogical University,
Yekaterinburg, Russia
e-mail: rin@imp.uran.ru

The microwave giant magnetoresistance effect in a (CoFe/Cu) superlattice with micron-sized holes has been studied. Measurements of the frequency dependences of the transmission coefficient, as well as the dependences of the microwave transmission and reflection coefficients on the magnetic field, are performed. The measurements were performed on the superlattice samples without holes, having one hole with a diameter of $6.3\,\mu$m and seven holes with a diameter of $1.7\,\mu$m. It is shown that the presence of a hole with a diameter of $6.3\,\mu$m leads to a significant frequency dependence of the microwave giant magnetoresistance effect. Magnetic and magnetoresistance measurements of superlattice samples were performed.

Keywords: metal superlattices, ferromagnetic resonance, ferromagnetic antiresonance, microwave giant magnetoresistance effect.

Introduction

The microwave giant magnetoresistance effect (μGMR) in metallic nanostructures has been discovered in [1] and later studied thoroughly in [2]. The technique of microwave transmission was applied in the study of μGMR, and a unique correspondence between the measured direct-current giant magnetoresistance effect (GMR) [3–5] and relative variations of the transmission coefficient of microwaves was established [6]. The theory of transmission of microwaves through a thin metal plate was developed in [7]. The transmission of microwaves through metallic nanostructures was examined for several classes of such nanostructures. It was found that the magnitude of the μGMR effect in multilayer Co/Cu structures is especially large [8,9]. High-frequency GMR was observed in [10] in experiments with high-frequency currents flowing perpendicularly to the layers of a superlattice. A series of studies were devoted to the examination of μGMR in a wave reflected from a nanostructure [11–13].

Magnonics is a relatively new trend in exploration of high-frequency properties of nanoobjects (specifically, laterally bounded films and nanostructures [14–20]). The problem of transmission of microwaves through a small (compared to the wavelength) hole in a metallic diaphragm is considered to be one of the classical problems of magnonics [21,22]. It was solved theoretically for a diaphragm positioned in a rectangular waveguide in [23]. These results were used in [24] in calculations for a Bethe directional coupler. It was found that the transmitted power increases abruptly if the medium in the hole has an unusual (near-zero) permittivity

value [25,26]. Magnetic and microwave properties in an array of holes („antidots") in a permalloy film were studied in [27]. The examination of ferromagnetic resonance (FMR) revealed the presence of bound magnetic states localized in the region of an individual hole. The transmission of tera-hertz radiation through a diaphragm with an array of holes was examined in [28]. It was found that two mechanisms of interaction between waves and inhomogeneities affect the characteristics of transmitted waves: (1) resonances associated with local characteristics of individual holes and the excitation of waves in their vicinity; (2) generation of fields from the entire array of holes as a sum of diffraction fields. Apart from magnonics, the problems of wave transmission and reflection in a system of periodic and aperiodic inhomogeneities (reflectors) are considered in research into sensors based on fiber Bragg gratings (FBGs) [29]. Nanostructures with a grooved surface are also used in magnetic and high-frequency sensors [30]. A grooved surface enhances the sensitivity of a sensor. The research in all related fields mentioned above is focused on the interaction of electromagnetic waves with nanoscale distortions of the surface or the bulk of films (or periodic structures). However, the purposes of this research and the frequency ranges of electromagnetic radiation differ from one field to the other.

The aim of the present study is to examine the influence of a single hole (or several holes) on the μGMR effect observed in an external magnetic field. A fraction of microwave power is transmitted trough holes, and the remaining power goes through the metal of a superlattice. If these two fractions of power are comparable, the

frequency dependence of μGMR changes as a result of interference. Since μGMR decreases when holes are present, it appears reasonable to choose nanostructures with large GMR magnitudes as samples for study. We have examined a (CoFe)/Cu superlattice system, which exhibits a very high magnetoresistance if the thickness of layers is chosen properly [31,32]. Another argument in favor of the (CoFe)/Cu superlattice system is that spin-wave resonances were observed in this system [33]. The problem addressed in the present study differs from the one being solved in FBG research, since we consider a metallic superlattice, while FBG systems are dielectric structures. The structure studied here also differs from nanostructures with a grooved surface, since through holes were made in the metallic nanostructure by dry etching in our experiments.

The results of examination of transmission of microwaves through a (CoFe)/Cu superlattice system without holes and through superlattice samples with a single micrometer hole and seven such holes are reported below. The frequency dependences of transmission coefficients are studied in the millimeter range at the frequencies of $26-38\,GHz$. The μGMR effect is measured at a number of frequencies.
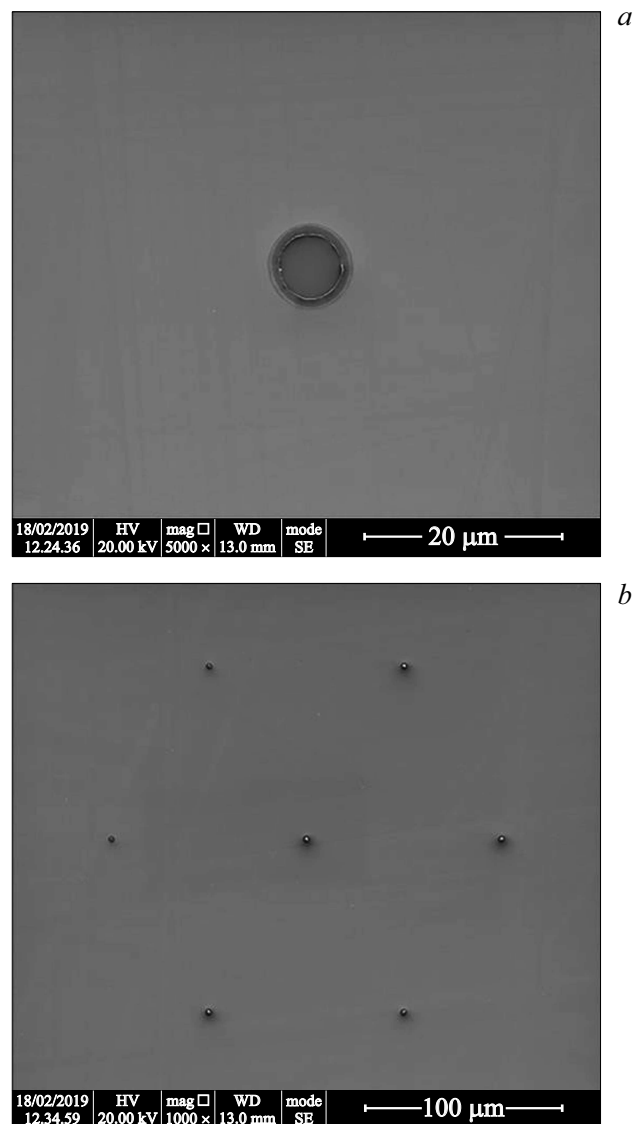
1. Samples and their characterization

An MPS-4000-C6 (ULVAC Inc., Japan) high-vacuum precision system was used to prepare $[(CoFe)/Cu]_n$ superlattices by magnetron sputtering. Superlattice samples had the following compositions: glass//Ta5.0/PyCr5.0/$[Co_{88}Fe_{12}1.5/Cu0.95]_{24}$/PyCr3.0 (sample No. 1) and glass//PyCr5.0/$[Co_{90}Fe_{10}1.5/Cu0.9]_{24}$/Ta3.0. The numbers following the layer composition in these designations correspond to the layer thickness, and indices next to square brackets denote the number of layers. Py is the $Fe_{20}Ni_{80}$ alloy, and PyCr is the paramagnetic $(Fe_{20}Ni_{80})_{60}Cr_{40}$ alloy. The Cu spacer thickness was chosen so that the sample would correspond to the first maximum of the dependence of the GMR magnitude on the spacer thickness. Samples were grown on Corning glass substrates with a thickness of $0.5\,mm$ (No. 1) and $0.2\,mm$ (the other samples). The procedure of growth of (CoFe)/Cu superlattices was detailed in [32]. The total thickness of metal in two superlattices is 66.8 and 65.6 nm.
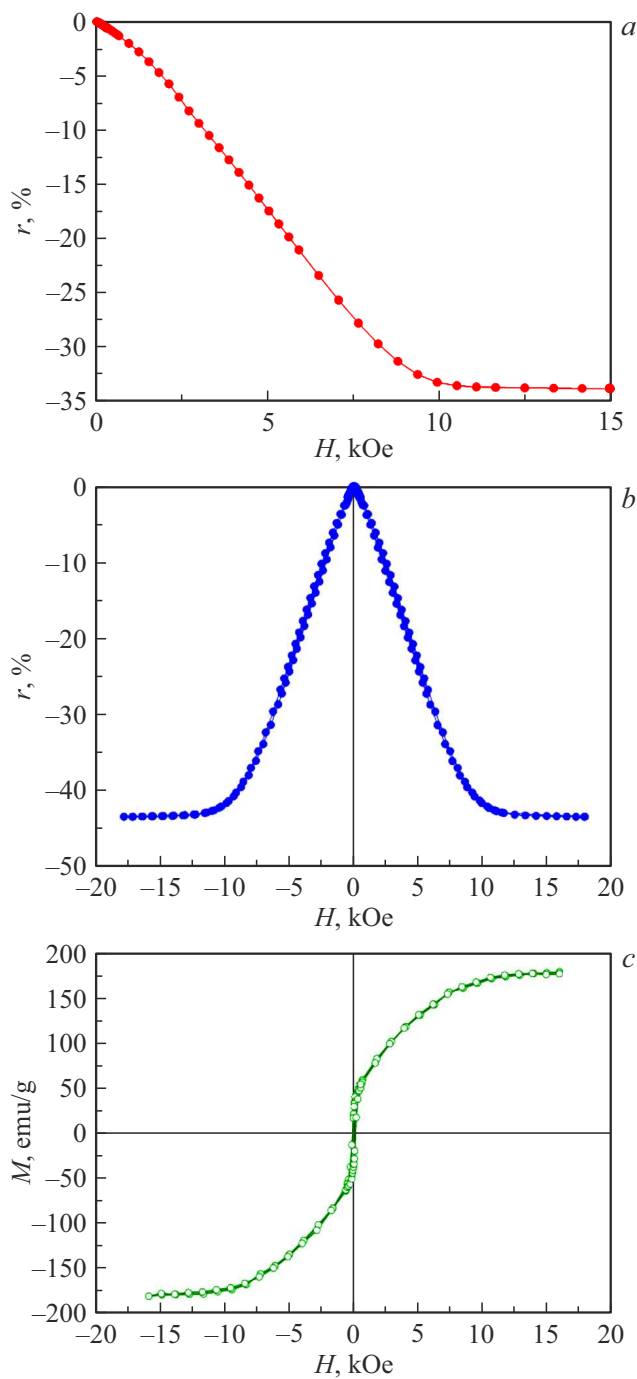
The X-ray examination of samples was conducted at the common use center of the Institute of Metal Physics of the Ural Branch of the Russian Academy of Sciences with the use of a PanAnalytical diffractometer. Both superlattices feature a peak from the family of planes (111) of the FCC lattice in the diffraction pattern. This peak is common to Cu and the CoFe alloy, since the parameters of the FCC lattice of copper and this alloy are very close. Oscillations around this peak were also observed. The superlattice period calculated based on the angular position of these oscillations agrees with the nominal values determined based on the growth rate and time. The lack of other characteristic peaks of the FCC lattice in the diffraction pattern suggests

that axial texture $\langle 111\rangle$ was formed in the samples. The technique of atomic force microscopy was used to study the surface relief of samples with a Solver Next (NT-MDT, Zelenograd) scanning probe microscope. It was found that the samples have a smooth surface with a height variation of approximately $3\,nm$ within a scan area of $1 \times 1\,\mu m$.

Through holes were made in glass//PyCr5.0/ $[Co_{90}Fe_{10}1.5/Cu0.9]_{24}$/Ta3.0 samples by dry etching: one hole $6.3\,\mu m$ in diameter in sample No. 2 and seven holes with a diameter of approximately $1.7\,\mu m$ in sample No. 3. The images of holes obtained using a scanning electron microscope are presented in Fig. 1. The hole diameter of $1.7\,\mu m$ is the smallest one that could be obtained with the available equipment for lithography and dry etching. The area of one such hole is very small compared to the area of the entire sample, and this hole cannot exert any

Figure 1. Electron microscope image of holes in superlattice samples: a — one hole $6.3\,\mu m$ in diameter in sample No. 2; b — seven holes with a diameter of approximately $1.7\,\mu m$ in sample No. 3. The accelerating voltage is $20\,kV$.

Figure 2. Magnetoresistance dependences for sample No. 1 (*a*) and samples Nos. 2 and 3 (*b*). The hysteresis loop for samples Nos. 2 and 3 (*c*).

capability taken into account). A hole $6.3\,\mu$m in diameter was made in sample No. 2. According to estimates, a hole of this size may alter the transmission of microwaves. This assumption was verified in subsequent experiments.

Direct-current magnetoresistance dependences were measured for the prepared samples (see Figs. 2, *a*, *b*). The saturation field of the magnetoresistance dependence for sample No. 1 is approximately 10 kOe, and relative magnetoresistance $r = [\rho(H) - \rho(0)]/\rho(0) \cdot 100\%$, where $\rho(H)$ is the electric resistance in magnetic field H, in saturation is -34%. The magnetoresistance dependence for samples Nos. 2 and 3 is shown in Fig. 2, *b*. The saturation field for these samples is also 10 kOe, and the maximum magnetoresistance in saturation is -43%. The error of magnetoresistance measurements is below 1%. It can be seen from Fig. 2, *b* that hysteresis has only a minor effect on the magnetoresistance dependence. The very large magnetoresistance of samples corresponds to the magnetic structure of layers with antiparallel ordering of moments of adjacent layers in zero external field. Figure 2, *c* shows the hysteresis loop in the measurement of magnetization of samples Nos. 2 and 3. Magnetic saturation is achieved in this measurement in fields of ~ 10 kOe.

2. Microwave measurements

Microwave measurements were performed at room temperature in the frequency range of 26–38 GHz. In these measurements, the sample is fitted into a frame constructed so as to prevent the leakage of electromagnetic energy at the sample edges. Holes are positioned at the centers of samples Nos. 2 and 3. The diagram of microwave measurements is presented in Fig. 3. Frame with sample *4* is introduced into rectangular waveguide *1* with a transverse size of 7.2×3.4 mm. The generator of the amplitude–frequency response meter excites a wave in the waveguide, and this wave reaches the sample. The amplitudes of reflected and transmitted waves are measured by the receiving

Figure 3. Diagram of microwave measurements: *1* — rectangular waveguide, *2* — electromagnet, *3* — directional couplers, *4* — sample, *5* — absorbers.
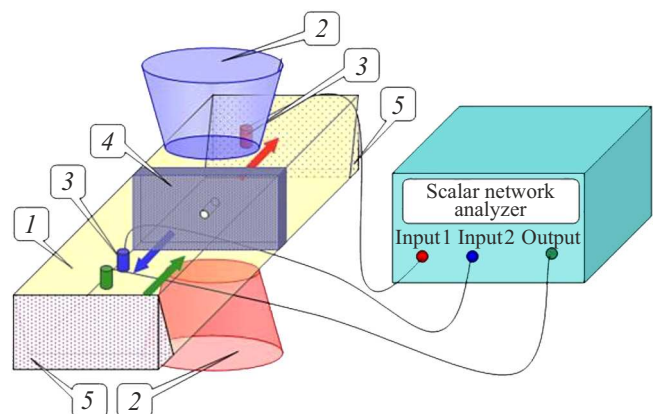
discernible influence on the microwave characteristics. Therefore, a system of seven holes with distance between them being much greater than the hole diameter was chosen for sample No. 3. With this positioning of holes, the distortion of microwave fields in the vicinity of any given hole does not extend over to the adjacent hole. A compact arrangement of holes near the center of the cross section of a waveguide was chosen (with the lithography equipment

section of the amplitude–frequency response meter with the use of directional couplers *3*. Absorbers *5* suppress the unwanted reflection from elements of the microwave pathway. An external magnetic field with an intensity up to 12 kOe is produced by electromagnet *2*. The magnitudes of transmission T and reflection R coefficients and their relative variations in the magnetic field are measured:

$$d_m = [|T(H)| - |T(0)|]/|T(0)| \cdot 100\%,$$

$$r_m = [|R(H)| - |R(0)|]/|R(0)| \cdot 100\%,$$

where $|T(H)|$ and $|R(H)|$ are the magnitudes of transmission and reflection coefficients in magnetic field H. Directional couplers of transmitted and reflected waves are positioned more than 20 cm away from the sample. Higher types of waves generated at the sample as a nonuniformity in the microwave pathway decay at such distances, and measurements are performed for the primary type of waves TE_{10}. The error of measurements of the transmission coefficient magnitude is $5-7\%$. The error of measurements of relative variation d_m of the transmission coefficient in a magnetic field does not exceed 3% of the measured value, and the corresponding error for measurements of refection coefficient variation r_m is no higher than 10%.

The results of measurements of the amplitude–frequency curves for transmission coefficients of samples in zero magnetic field are presented in Fig. 4. It can be seen that seven holes with a diameter of $1.7\,\mu$m have only a slight effect on the amplitude–frequency curve. The transmission coefficient of the sample with a hole $6.3\,\mu$m in diameter increases by a factor of approximately 1.5. These results may be interpreted in the following way: the major part of microwave power in sample No. 3 is transmitted through the metal of the superlattice, while the fractions of microwave power transmitted through the metal and the hole in sample No. 2 are comparable.

Let us turn to the examination of the μGMR effect in a magnetic field. The results of measurements of the field
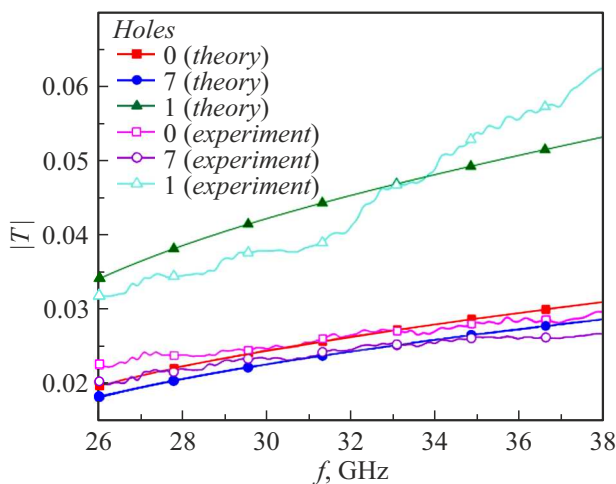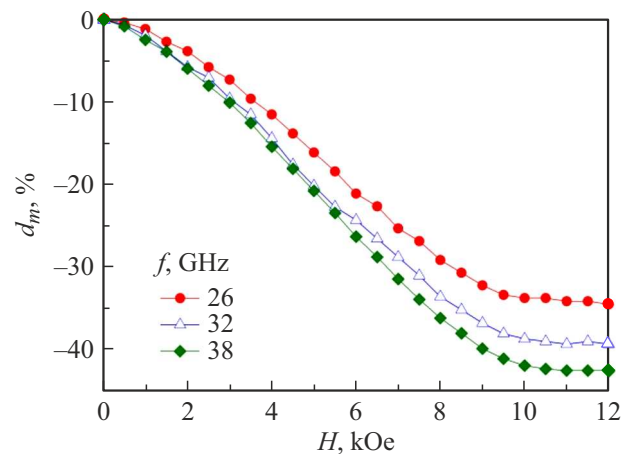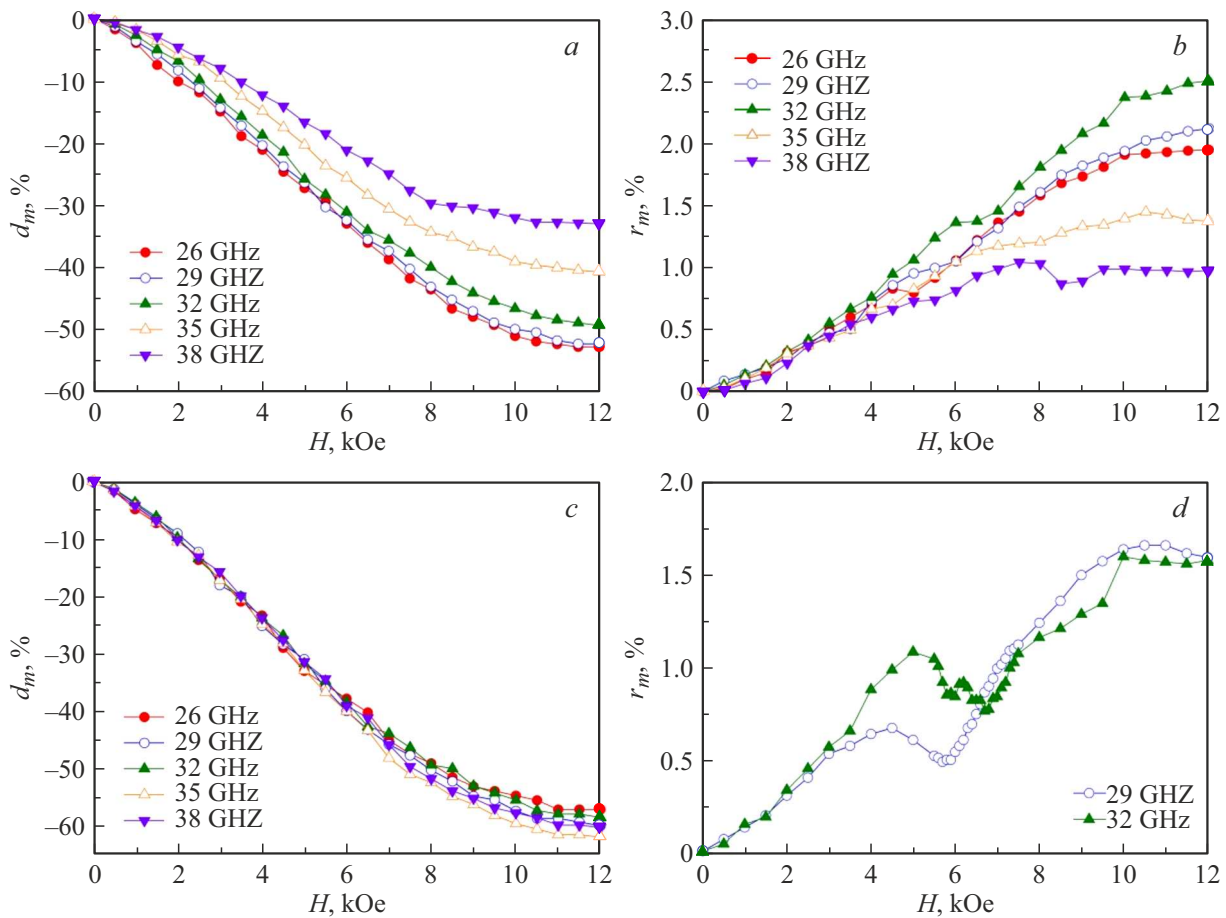

Figure 5. Dependence of the transmission coefficient on the magnetic field for sample No. 1 without holes measured at several frequencies of the millimeter range.

dependence of the microwave transmission coefficient for sample No. 1 without holes are presented in Fig. 5. In accordance with [6], the microwave dependences are similar in general to the dependence of the relative magnetoresistance. However, there are certain differences. First, the maximum magnitude of microwave variations is $15-25\%$ higher than GMR. This feature of the (CoFe)/Cu system has already been noted in [33]. According to the results of analysis performed there, this difference is likely attributable to the fact that the effective medium approximation, which was used to derive a unique correspondence in [6], is only partially suitable for a multilayer nanostructure. The second difference consists in the fact that the maximum μGMR value has a certain dependence on frequency.

Figure 6 shows the magnetic-field dependences of transmission and reflection coefficients measured in samples Nos. 2 and 3 with holes. Let us compare the results of measurements of transmission coefficients in samples Nos. 2 and 3. As was demonstrated above (in measurements in zero magnetic field), the fractions of microwave power transmitted through the hole and the metal of the superlattice in sample No. 2 with one large-diameter hole are comparable. In sample No. 3, microwave power is transmitted primarily by the wave that passes through the metal of the superlattice. In both cases, the dependences of microwave transmission and the relative magnetoresistance of the sample are qualitatively similar. Just as in sample No. 1 without holes, the magnitude of microwave variations is somewhat higher than the relative magnetoresistance. However, sample No. 2 with one hole $6.3\,\mu$m in diameter features a well-pronounced frequency dependence of the maximum variations of the transmission coefficient.

Let us compare the results of measurements of the field dependence of reflection coefficients. As is known, variations of the reflection coefficient in the μGMR effect are positive in sign, are similar in shape to the relative

Figure 4. Amplitude–frequency curves of samples Nos. 1 (without holes), 2 (with one hole), and 3 (with seven holes).

Figure 6. Magnetic-field dependences of transmission (a, c) and reflection (b, d) coefficients for sample No. 2 with one hole $6.3\,\mu$m in diameter (a, b) and sample No. 3 with seven holes with a diameter of $1.7\,\mu$m (c, d) measured at several frequencies of the millimeter range.

magnetoresistance, and are much smaller than it in magnitude [12]. In the case of sample No. 2 with one hole $6.3\,\mu$m in diameter, a well-pronounced frequency dependence of the maximum microwave variations, which is similar to the one for the transmission coefficient, is evident. A maximum caused by the ferromagnetic antiresonance (FMAR) and a minimum due to the absorption of microwaves, which occurs when the FMR condition is satisfied, are observed for sample No. 3 with seven holes with a diameter of $1.7\,\mu$m against the background of a monotonic increase of the reflection coefficient due to the μGMR effect [34].

3. Discussion

The coefficients of transmission and reflection of microwaves may be calculated in the continuous medium approximation, where a multilayer metallic nanostructure is substituted with a homogeneous plate of the same thickness with effective conductivity and permeability values. According to [35–37], coefficients of transmission T and reflection R of an electromagnetic wave are expressed as

follows in this approximation:

$$T = \frac{2Z_m}{2Z_m\,\mathrm{ch}\,k_m d + Z\,\mathrm{sh}\,k_m d}, \tag{1}$$

$$R = -1 + \frac{2Z_m\,\mathrm{ch}\,k_m d}{2Z_m\,\mathrm{ch}\,k_m d + Z\,\mathrm{sh}\,k_m d}, \tag{2}$$

where $k_m = (1 + i)/\delta$ is the wave number in a conductive medium with normal skin effect and d is the overall metal thickness in the nanostructure (i.e., total thickness of all metal layers). The nanostructure impedance is $Z_m = (1 + i)\rho/\delta$, where $\rho = \rho(H)$ is the resistivity of the nanostructure, $\delta = \sqrt{2\rho/\omega\mu\mu_0}$ is the skin layer depth, $\omega = 2\pi f$ is the circular frequency, and μ is the relative dynamic differential permeability. Note that formulae (1) and (2) were derived under the assumption [35] that the dependences on time and spatial coordinate for the corresponding electromagnetic waves propagating in positive and negative directions along, say, axis y have the form of $\exp(i\omega t - k_m y)$ and $\exp(i\omega t + k_m y)$.
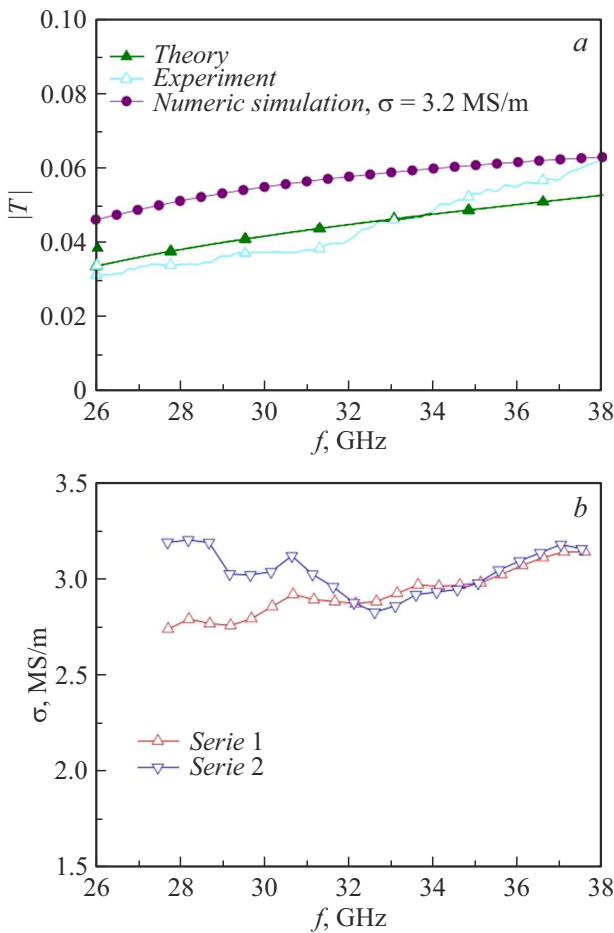
Figure 7. Comparison of the amplitude–frequency dependences of the transmission coefficient for sample No. 2 that were measured, calculated in accordance with (1), and calculated in ANSYS HFSS (*a*); frequency dependences of the effective conductivity of samples Nos. 2 and 3 (*b*).

With a TE$_{10}$-type wave, the impedance of the waveguide containing the nanostructure is calculated as

$$Z = \sqrt{\frac{\mu_0/\varepsilon_0}{1 - (\lambda/\lambda_c)^2}}, \qquad (3)$$

where $\lambda = c/f$ is the wavelength in vacuum, $\lambda_c = 2a$ is the critical wavelength of mode TE$_{10}$, and a is the size of the larger wall of a rectangular waveguide. In our experiments, $a = 7.2$ mm. Impedance Z_m of a highly conductive nanostructure is lower than waveguide impedance Z, $|Z_m| \ll Z$. We consider formulae (1) and (2) in the limit case of $d \ll \delta$ that is relevant to millimeter wavelengths. Then $2Z \operatorname{ch} k_m d \ll Z \operatorname{sh} k_m d$, and the transmission and reflection coefficients are given by

$$T = \frac{2Z_m}{Z \operatorname{sh} k_m d}, \qquad (4)$$

$$R = -1 + \frac{2Z_m}{Z} \operatorname{cth} k_m d. \qquad (5)$$

Figure 7, *a* presents the comparison of dependences of the transmission coefficient for sample No. 2 that were measured, calculated in accordance with Eq. (1), and determined numerically in ANSYS HFSS. The frequency dependences of the effective conductivity of samples were derived by analyzing thoroughly the frequency dependences of transmission and reflection coefficients of samples Nos. 2 and 3. The obtained dependences are shown in Fig. 7, *b*. As was expected, the variations of conductivity of superlattices with frequency are insignificant.

The magnetic-field dependences of the microwave transmission coefficient calculated in accordance with Eq. (1) and measured experimentally for sample No. 3 with seven holes with a diameter of $1.7\,\mu$m were compared (Fig. 8). While these dependences are similar in shape and represent like-sign variations of the transmission coefficient, significant differences between the calculated and measured data should be noted. First, the calculated magnitude of variations of the microwave coefficient is exactly equal to the measured direct-current GMR effect. Experimental microwave dependences reveal variations that are $1.3-1.4$ times greater in magnitude. Second, calculated data are almost independent of frequency, while measured data feature such a dependence.

Let us specify the adopted approximations that may account for the difference between calculated and measured data. The multilayer nanostructure with layers of different materials was substituted in calculations with a homogeneous plate of the same thickness with equivalent parameters. AS was demonstrated in [33], this approximation is only partially applicable to the (CoFe)/Cu system with a very large magnetoresistance. At the same time, adequate results were obtained in [6,12] for the Fe/Cr system with a moderate magnetoresistance.

The second significant approximation is the neglected influence of the dielectric substrate in calculations. This
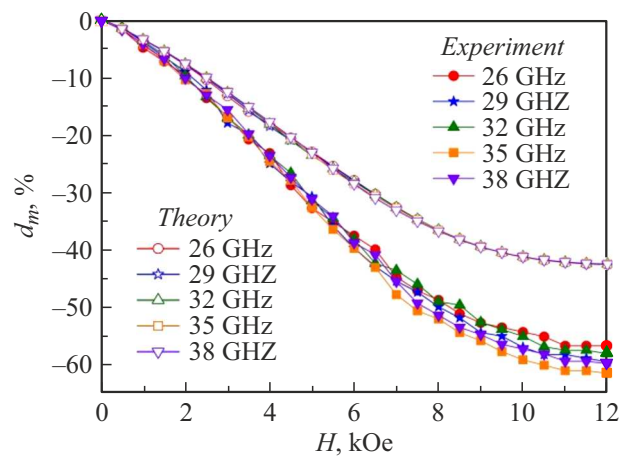
Figure 8. Magnetic-field dependences of the microwave transmission coefficient calculated in accordance with Eq. (1) and measured experimentally for sample No. 3 with seven holes with a diameter of $1.7\,\mu$m.

is justified by the fact that nonuniformities introduced into the microwave pathway by the metal of the superlattice are much more substantial than those of the dielectric substrate. In addition, the substrate is fairly thin. It is considerably thinner than a quarter- or a half-wave plate.

The results of calculations with these approximations reveal a unique correspondence between GMR and μGMR and an almost complete lack of the frequency dependence of variations of the microwave transmission coefficient. These specific features persist in calculations for nanostructures with a widely varying overall metal thickness (from several nanometers to several tens of micrometers) and within a wide frequency interval from centimeter to millimeter waves. Thus, there are reasons to believe that the mentioned differences between calculated and experimental data are related to the discussed approximations.

Conclusion

The electrodynamic characteristics of (CoFe)/Cu super-lattices with micrometer-sized holes were considered. The amplitude–frequency curves and the microwave transmission and reflection coefficients in a magnetic field were measured. Direct-current magnetoresistance characteristics were also measured. The effective microwave conductivity of superlattice samples was determined.

The microwave giant magnetoresistance effect was examined in superlattices with one hole and seven holes. It was found that a hole $6.3\,\mu$m in diameter induces a significant frequency dependence of μGMR both in transmission and in reflection of microwaves. The maximum variation of amplitude of the transmitted wave changes by a factor of more than 1.5 within the frequency interval of 26–38 GHz. Seven holes with a diameter of $1.7\,\mu$m in the sample do not induce any noticeable μGMR dispersion. Resonance-type variations caused by FMR and FMAR were observed for this sample in the reflected signal.

Conflict of interest

The authors declare that they have no conflict of interest.

References

[1] J.J. Krebs, P. Lubitz, A. Chaiken, G.A. Prinz. J. Appl. Phys., **69** (8), 4795 (1991). DOI: 10.1063/1.348232

[2] B.K. Kuanr, A.V. Kuanr, P. Grünberg, G. Nimtz. Phys. Lett. A, **221** (3–4), 245 (1996). DOI: 10.1016/0375-9601(96)00567-1

[3] M.N. Baibich, J.M. Broto, A. Fert, F. Nguyen Van Dau, F. Petroff, P. Eitenne, G. Creuzet, A. Friederich, J. Chazelas. Phys. Rev. Lett., **61** (21), 2472 (1988). DOI: 10.1103/PhysRevLett.61.2472

[4] G. Binasch, P. Grünberg, F. Saurenbach, W. Zinn. Phys. Rev. B, **39** (7), 4828 (1989). DOI: 10.1103/PhysRevB.39.4828

[5] P. Bruno. Phys. Rev. B, **52** (1), 411 (1995). DOI: 10.1103/PhysRevB.52.411

[6] V.V. Ustinov, A.B. Rinkevich, L.N. Romashev, V.I. Minin. JMMM, **177**–**181**, 1205 (1998). DOI: 10.1016/S0304-8853(97)00279-5

[7] E.M. Kogan, E.A. Turov, V.V. Ustinov. Phys. Met. Metallogr., **53** (2), 223 (1982).

[8] T. Rausch, T. Szczurek, M. Schlesinger. J. Appl. Phys., **85** (1), 314 (1999). DOI: 10.1063/1.369448

[9] D.P. Belozorov, V.N. Derkach, S.V. Nedukh, A.G. Ravlik, S.T. Roschenko, I.G. Shipkova, S.I. Tarapov, F. Yildiz. Int. J. Infrared Milli. Waves, **22** (11), 1669 (2001). DOI: 10.1023/A:1015060515794

[10] V.V. Ustinov, A.B. Rinkevich, L.N. Romashev. JMMM, **198**–**199**, 82 (1999). DOI: 10.1016/S0304-8853(98)00631-3

[11] Z. Frait, P. Šturc, K. Temst, Y. Bruynseraede, I. Vávra. Solid State Commun., **112** (10), 569 (1999). DOI: 10.1016/S0038-1098(99)00392-0

[12] V.V. Ustinov, A.B. Rinkevich, L.N. Romashev, E.A. Kuznetsov. Tech. Phys., **54** (8), 1156 (2009). DOI: 10.1134/S1063784209080106

[13] D.E. Endean, J.N. Heyman, S. Maat, E. Dan Dahlberg. Phys. Rev. B, **84** (21), 212405 (2011). DOI: 10.1103/PhysRevB.84.212405

[14] A.V. Chumak, V.I. Vasyuchka, A.A. Serga, B. Hillebrands. Nat. Phys., **11** (6), 453 (2015). DOI: 10.1038/nphys3347

[15] B. Divinskiy, V.E. Demidov, S.O. Demokritov, A.B. Rinkevich, S. Urazhdin. Appl. Phys. Lett., **109** (25), 252401 (2016). DOI: 10.1063/1.4972244

[16] S.A. Nikitov, D.V. Kalyabin, I.V. Lisenkov, A.N. Slavin, Yu.N. Barabanenkov, S.A. Osokin, A.V. Sadovnikov, E.N. Beginin, M.A. Morozova, Yu.P. Sharaevsky, Yu.A. Filimonov, Yu.V. Khivintsev, S.L. Vysotsky, V.K. Sakharov, E.S. Pavlov. Phys. Usp., **58** (10), 1002 (2015). DOI: 10.3367/UFNe.0185.201510m.1099

[17] A. Fert. Phys. Usp., **51** (12), 1336 (2008). DOI: 10.3367/UFNr.0178.200812f.1336

[18] M. Farle, T. Silva, G. Woltersdorf. In: *Magnetic Nanostructures, Spin Dynamics and Spin Transport,* ed. by H. Zabel, M. Farle. (Springer-Verlag, Berlin, Heidelberg, 2013), p. 37. DOI: 10.1007/978-3-642-32042-2

[19] X. Zhang, W. Butler. In: *Handbook of Spintronics,* ed. by Y. Xu, D.D. Awschalom, J. Nitta. (Springer, Dordrecht, Heidelberg, NY., London, 2016), p. 3. DOI: 10.1007/978-94-007-6892-5

[20] *Ultrathin Magnetic Structures,* ed. by B. Heinrich, J.A.C. Bland. (Springer, Berlin Heidelberg, NY., 2005), v. IV. DOI: 10.1007/b138704

[21] R.E. Collin. *Field Theory of Guided Waves* (Wiley-Interscience-IEEE, NY., Chichester, Weinheim, Brisbane, Singapore, Toronto, 1991)

[22] M. Skorobogatiy. *Nanostructured and Subwavelength Waveguides: Fundamentals and Applications* (John Wiley & Sons, Chichester, 2012)

[23] N. Marinescu. Phys. Rev. E, **56** (2), 2166 (1997). DOI: 10.1103/PhysRevE.56.2166

[24] N. Marinescu. Phys. Rev. E, **54** (3), 2931 (1996).
DOI: 10.1103/PhysRevE.54.2931

[25] M.G. Silveirinha, N. Engheta. Phys. Rev. Lett., **97** (15),
157403 (2006). DOI: 10.1103/PhysRevLett.97.157403

[26] S.A. Maier. *Plasmonics: Fundamentals and Applications*
(Springer Science + Business Media LLC, NY., 2007),
DOI: 10.1007/0-387-37825-1

[27] A.S. Silva, A. Hierro-Rodriguez, S.A. Bunyaev, G.N. Kakazei,
O.V. Dobrovolskiy, C. Redondo, R. Morales, H. Cre-
spo, D. Navas. AIP Advances, **9** (3), 035136 (2019).
DOI: 10.1063/1.5080111

[28] V. Lomakin, S. Li, E. Michielssen. Microw. Opt. Technol. Lett.,
49 (7), 1554 (2007). DOI: 10.1002/mop.22484

[29] A. Othonos, K. Kalli. *Fiber Bragg Gratings: Fundamen-*
tals and Applications in Telecommunications and Sensing
(Artech House, Norwood, 1999)

[30] Y. Mu, P. Li, Y. Wen. IEEE Sens. J., **21** (20), 22623 (2021).
DOI: 10.1109/JSEN.2021.3110870

[31] W. Kuch, A.C. Marley, S.S.P. Parkin. J. Appl. Phys., **83** (9),
4709 (1998). DOI: 10.1063/1.367259

[32] M.A. Milyaev, L.I. Naumova, V.V. Ustinov. Phys. Met.
Metallogr., **119** (12), 1162 (2018).
DOI: 10.1134/S0031918X1812013X

[33] V.V. Ustinov, A.B. Rinkevich, I.G. Vazhenina, M.A. Milyaev.
JETP, **131** (1), 139 (2020).
DOI: 10.1134/S1063776120070171

[34] V.V. Ustinov, A.B. Rinkevich, D.V. Perov, A.M. Burkhanov,
M.I. Samoylovich, S.M. Kleshcheva, E.A. Kuznetsov. **58** (4),
568 (2013). DOI: 10.1134/S1063784213040257

[35] N.A. Semenov. *Tekhnicheskaya elektrodinamika* (Svyaz', M.,
1972) (in Russian).

[36] L.M. Brekhovskikh. *Waves in Layered Media* (Academic
Press, London, 1980)

[37] L.F. Chen, C.K. Ong, C.P. Neo, V.V. Varadan, V.K. Varadan.
Microwave Electronics: Measurement and Materials
Characterization (John Wiley & Sons, Hoboken, 2004),
DOI: 10.1002/0470020466